Development 128, 155-166 (2001)
Printed in Great Britain © The Company of Biologists Limited 2001
DEV3232

The forkhead transcription factor Foxf1 is required for differentiation of extra-embryonic and lateral plate mesoderm

Margit Mahlapuu[1], Mattias Ormestad[1], Sven Enerbäck[2] and Peter Carlsson[1,*]

[1]Department of Molecular Biology, Göteborg University, The Lundberg Laboratory, Medicinaregatan 9C, Box 462, S-405 30 Göteborg, Sweden
[2]Department of Medical Biochemistry, Göteborg University, Medicinaregatan 9C, S-405 30 Göteborg, Sweden
*Author for correspondence (e-mail: peter.carlsson@molbio.gu.se)

Accepted 30 October; published on WWW 21 December 2000

SUMMARY

The murine *Foxf1* gene encodes a forkhead transcription factor expressed in extra-embryonic and lateral plate mesoderm and later in splanchnic mesenchyme surrounding the gut and its derivatives. We have disrupted *Foxf1* and show that mutant embryos die at midgestation due to defects in mesodermal differentiation and cell adhesion. The embryos do not turn and become deformed by the constraints of a small, inflexible amnion. Extra-embryonic structures exhibit a number of differentiation defects: no vasculogenesis occurs in yolk sac or allantois; chorioallantoic fusion fails; the amnion does not expand with the growth of the embryo, but misexpresses vascular and hematopoietic markers. Separation of the bulk of yolk sac mesoderm from the endodermal layer and adherence between mesoderm of yolk sac and amnion, indicate altered cell adhesion properties and enhanced intramesodermal cohesion. A possible cause of this is misexpression of the cell-adhesion protein VCAM1 in *Foxf1*-deficient extra-embryonic mesoderm, which leads to co-expression of VCAM with its receptor, α_4-integrin. The expression level of *Bmp4* is decreased in the posterior part of the embryo proper. Consistent with this, mesodermal proliferation in the primitive streak is reduced and somite formation is retarded. Expression of *Foxf1* and the homeobox gene *Irx3* defines the splanchnic and somatic mesodermal layers, respectively. In *Foxf1*-deficient embryos incomplete separation of splanchnic and somatic mesoderm is accompanied by misexpression of *Irx3* in the splanchnopleure, which implicates *Foxf1* as a repressor of *Irx3* and as a factor involved in coelom formation.

Key words: Foxf1, Forkhead, Allantois, Yolk sac, Amnion, Lateral mesoderm, Mouse

INTRODUCTION

The body plan of the vertebrate embryo is established during gastrulation by the formation of mesoderm, separating the ectodermal and endodermal germ layers. Embryonic mesoderm, formed in the primitive streak, migrates anteriorly and is divided along the mediolateral axis into distinct populations including axial, paraxial, intermediary and lateral plate mesoderm. The antagonistic activities of BMP4 and noggin control mediolateral differentiation of mesoderm and high BMP4 signaling promotes lateral plate formation (Tonegawa et al., 1997; Tonegawa and Takahashi, 1998). The lateral plate is further subdivided into somatopleure and splanchnopleure by a split in the mesoderm which creates the coelom, or body cavity. Cues provided by the ectoderm and endoderm induce subdivision of the lateral plate and ectodermal BMP signaling (BMP2 and/or BMP7) has been implicated in this process (Funayama et al., 1999).

Mesoderm also contributes to extra-embryonic structures such as amnion, allantois and yolk sac. The amnion, which is the extra-embryonic extension of the somatopleure, is a thin membrane that encloses the embryo. It consists of two connected monolayers of flattened cells, one mesodermal and one ectodermal. The composition of the amniotic fluid is determined by active transport of metabolites across the amnion and damage to this barrier will disturb embryonic development (Chang et al., 1996). The allantois is a mesodermal structure formed as an outgrowth from the posterior primitive streak. Originally an adaptation to terrestrial life in oviparous animals, the allantois in mammals forms the blood vessels of the umbilical cord and provides the embryonic link to the placenta through fusion with the chorion (Downs, 1998). Vascularization of the allantois is the result of de novo blood vessel formation (vasculogenesis), which begins in its distal part (Downs et al., 1998) and requires VEGF signaling through the receptor, Flk1 (Kdr; Shalaby et al., 1995). The fusion of chorion and allantois is essential for placentation and is mediated by α_4-integrin on chorion cells binding to vascular cell adhesion molecule (VCAM1) on the distal allantoic cells (Gurtner et al., 1995; Kwee et al., 1995; Yang et al., 1995).

The mammalian yolk sac is another evolutionary legacy from embryonic development inside an egg. It consists of an endodermal and a mesodermal layer, and is continuous with

the splanchnopleure of the embryo proper. In mammals, the yolk sac has lost its role as energy depot, but serves an important function in transport of nutrients, excretion products and gases during early development. Before the establishment of a circulation that links the embryo to the placenta, metabolites are exchanged through the yolk sac vasculature and the exocoelomic fluid. The yolk sac is also the initial site of hematopoiesis and provides the nucleated red blood cells that are the first to colonize the embryonic vasculature. Vasculogenesis and hematopoiesis take place in the mesodermal blood islands, followed by vascular remodeling and sprouting (angiogenesis) to form the arterial and venous trees (Risau and Flamme, 1995). This process requires VEGF signaling from the yolk sac endoderm (Ferrara et al., 1996) and VEGF receptors (Flk1 and Flt1) in the mesoderm which promote vascular morphogenesis and differentiation of endothelial and hematopoietic cells (Fong et al., 1995; Fong et al., 1999; Shalaby et al., 1995; Yamaguchi et al., 1993). Angiogenesis and differentiation of other vascular cell types, such as vascular smooth muscle cells, require additional related tyrosine kinase receptors (Sato et al., 1995). Close contact between the mesodermal and endodermal layers of the yolk sac is essential for VEGF signaling and normal vascular development. This association depends on deposition of the extracellular matrix component fibronectin (George et al., 1993) and expression of its major receptor, α_5/β_1-integrin, on mesodermal cells (Yang et al., 1993). TGFβ1 signaling is also necessary for mesodermal-endodermal adherence (Dickson et al., 1995; Oshima et al., 1996), which has been proposed to be mediated through regulation of fibronectin deposition (Goumans et al., 1999). Homophilic cell adhesion proteins are required for formation and remodeling of the vasculature; absence of N- or VE-cadherin causes yolk-sac vascularization defects without affecting the primary differentiation of vascular cell types (Carmeliet et al., 1999; Radice et al., 1997).

The gene *Foxf1*, previously known as *FREAC-1* or *HFH-8* (Pierrou et al., 1994; Hellqvist et al., 1996; Clevidence et al., 1994), encodes a forkhead, or winged helix, transcription factor that is expressed in mesodermal tissues. Expression can be detected from the primitive streak stage (Peterson et al., 1997) and during organogenesis it is mainly found in mesenchyme adjacent to the endodermal epithelia of the gastrointestinal tract, the airways and the urinary tract (Aitola et al., 2000; Mahlapuu et al., 1998; Peterson et al., 1997). In adults the principal site of expression is in lung and during pregnancy it is highly expressed in placenta (Pierrou et al., 1994). Here we have investigated the function of *Foxf1* during embryonic development by targeting the gene in mice.

MATERIALS AND METHODS

Targeting the *Foxf1* locus

A targeting construct containing a total of 12 kb of the *Foxf1* locus was made from overlapping 129/Sv genomic λ clones. The forkhead box of *Foxf1* (from *Sst*I to *Not*I) was replaced by a PGK-Neo cassette and the HSV-tk gene was appended to the short arm of the construct for negative selection. The construct was linearized at an *Sfi*I site inserted at the end of the long arm and electroporated into two embryonic stem (ES) cell lines: RW4, derived from 129/Sv, and E14, derived from 129/Ola. Colonies resistant to 300 μg/ml G-418 and 2 μM ganciclovir were screened by PCR with one primer (CTG CGC CCC GCA TCA TCT CTC CAA) located outside (upstream) of the short arm and the other (GCC CAG CCC GTT CAC CAT GCT GTA) downstream of the forkhead box. Recombination between the targeting construct and the *Foxf1* locus occurred with a frequency of 0.5% and was identified by the presence of a PCR product longer than the wild-type product. Homologous recombination was verified by Southern blot and hybridization with two probes. The first probe is located outside the short arm of the targeting construct and identifies fragments beginning at an external *Dra*I site and ending at *Dra*I sites downstream of the forkhead box (wt allele, 4 kb) or within the PGK-neo cassette (targeted allele, 2 kb). The other probe is located within the long arm and identifies fragments between an external *Hin*dIII site on the long arm side and *Eco*RV sites upstream of the short arm (wt allele, 15 kb) or within the PGK-neo cassette (targeted allele, 12 kb). Targeted cell clones were used to generate chimeras through injection of C57Bl/6 blastocysts (RW4) or aggregation with CD1 morulas (E14). Germline transmission was obtained with one clone derived from each cell line and the targeted allele was maintained on mixed 129/Ola-C57Bl/6, 129/Ola-CD1 and 129/Sv-C57Bl/6 backgrounds. Genotyping of tail biopsies or embryos was performed by Southern blot or by triplex PCR using a common primer located downstream of the forkhead box (GCC CAG CCC GTT CAC CAT GCT GTA), a primer specific for the forkhead box of the wt allele (TCG CGC TCA TCG TCA TGG CTA TCC) and a primer in the PGK promoter specific for the targeted allele (GGA GGA GTA GAA GTG GCG CGA AGG).

In situ hybridization, immunohistochemistry and histology

In situ hybridization of whole-mount embryos, cryosections (8 μm) and paraffin sections (4 μm) was performed as previously described (Blixt et al., 2000), using digoxigenin labeled RNA probes. The *Foxf1* probe corresponds to a 400 bp *Not*I/*Ksp*I cDNA fragment located immediately 3′ of the forkhead box. Plasmids used to generate probes for *Flk1* were kindly provided by Dr T. Yamaguchi (Samuel Lunenfeld Research Institute, Mount Sinai Hospital, Canada), for *Bmp4* by Dr B. L. M. Hogan (Howard Hughes, Nashville, USA), for *T* (*Brachyury*) by Dr B. G. Herrmann (Max-Planck-Institute for Immunobiology, Germany) for *Meox1* (formerly *Mox1*) by Dr J. M. Partanen (University of Helsinki, Finland), and for *Tbx2* by Dr R. J. Bollag (Institute of Molecular Medicine and Genetics, Medical Collage of Georgia, USA). Probes for vascular smooth muscle α-actin (*Actvs*) were generated from mouse IMAGE cDNA clone 1224519, for ζ-globin (*Hba-x*) from IMAGE cDNA clone 1261153, for iroquois-related homeobox 3 (*Irx3*) from IMAGE cDNA clone 1245751 and for transforming growth factor β1 (*Tgfb1*) from IMAGE clone 890715. Immunostainings were performed with antibodies to platelet/endothelial cell adhesion molecule (Pecam; Pharmingen, clone MEC 13.3), fibronectin 1 (Fn1; Biogenesis), α_4-integrin (Itga4; Pharmingen, clone R1-2), α_5-integrin (Itga5; Pharmingen, clone MFR5), VE-cadherin (Cdh5; Pharmingen, clone 11D4.1), N-cadherin (Cdh2; Zymed, clone NCD-2), E-cadherin (Cdh1; Pharmingen) and vascular cell adhesion molecule 1 (Vcam1; Pharmingen, clone MVCAM.A). Antibody binding was detected with biotinylated secondary antibodies and streptavidine-HRP amplified by TSA TM Biotin System (NEN Life Science Products) or Vectastain ABC Elite Kit (Vector Labs). Histological sections were stained with Hematoxylin and Eosin.

TUNEL and BrdU-incorporation assays

Apoptotic cells were identified with the TUNEL assay on 8 μm cryosections of embryonic day (E) 8.5 embryos (eight to ten pairs of somites) using terminal deoxynucleotidyltransferase, Biotin-16-dUTP (Boehringer Roche) and Cy3-conjugated streptavidine (Jackson ImmunoResearch). Nuclei were counterstained with DAPI (Sigma).

Since embryonic BrdU uptake following intraperitoneal injection of the pregnant female is very inefficient in embryos that have not established a placental-embryonic circulation (which occurs around E9 in wild-type embryos and not at all in *Foxf1* mutants), we

performed BrdU labeling in vitro. Whole concepti (E8.5; 9-11 pairs of somites) were dissected free from the decidua, holes were ripped in yolk sac and amnion to allow efficient entry of the culture medium and the concepti were incubated for 1 hour at 37°C, 5% CO_2 in Dulbecco's modified Eagle's medium supplemented with 100 μM BrdU (Sigma). Following fixation in 4% paraformaldehyde, concepti were cryosectioned (8 μm) and sections were incubated with anti-BrdU antibody (Becton Dickinson, Clone 3D4). Antibody binding was detected with a rabbit anti-mouse biotin-conjugated secondary antibody (Dako) and streptavidine-HRP amplified by TSA TM Biotin System (NEN Life Science Products). Nuclei were counterstained with Richardson's Azur-11-Methylene Blue. BrdU-positive and -negative nuclei were counted in posterior primitive streak mesoderm and neural plate in the same region. Mesodermal nuclei were counted on 14 sections (4725 nuclei in total) derived from eight embryos (four wild type and four null) and neuroectodermal nuclei on eight sections from the same embryos. Averages were compared using a two-tailed *t*-test.

Semi-quantitative RT-PCR assay

To compare the expression levels of *Vegf* and endothelial tyrosine kinase receptors in different genotypes, mRNA from E8.5 concepti was captured on oligo-dT-Dynabeads (Dynal, Norway) and converted to cDNA with AMV reverse transcriptase (Boehringer Roche, Germany). DNA recovered from the supernatant was used for PCR genotyping. Multiplex PCR was performed on the cDNA beads in the presence of α^{32}P-dATP; aliquots were taken out after 24, 26 and 28 cycles and separated by polyacrylamide gel electrophoresis. The amplified products were cut out, quantified in a scintillation counter and normalized against β-actin (*Actb*). β-actin primers were added after five cycles to compensate for the higher expression level. Averages of the ratios from the three aliquots were calculated for each conceptus and each amplification product; these values were used to calculate the combined average from ten (+/–) or six (–/–) concepti.

RESULTS

Embryonic expression of *Foxf1*

At the ninth day of gestation (E8.5) expression of *Foxf1* was localized to mesoderm of the posterior primitive streak, the lateral plate of the embryo proper and in the extra-embryonic mesoderm of allantois, amnion and yolk sac (Fig. 1A-F, Peterson et al., 1997). As differentiation of the lateral plate proceeded along the anteroposterior axis, *Foxf1* was turned off in the somatopleure, but remained expressed in the mesodermal

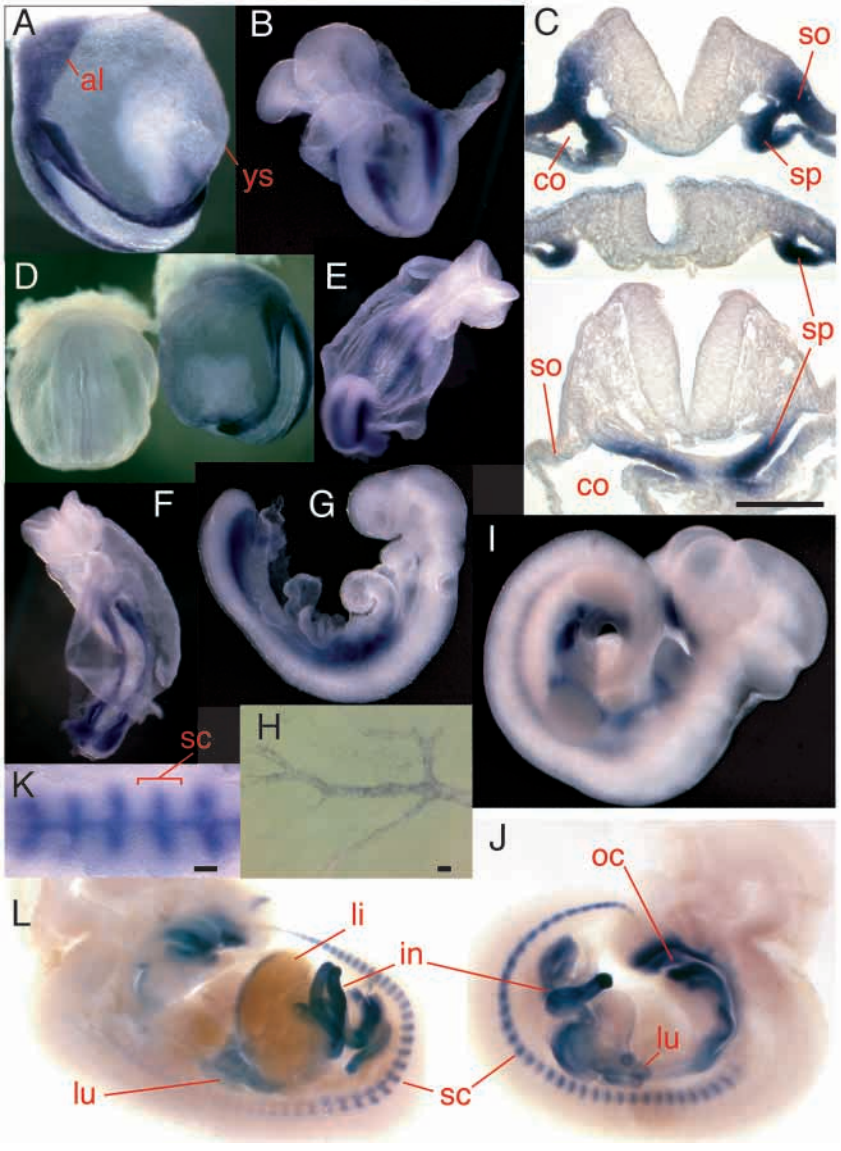

Fig. 1. Whole-mount in situ hybridizations showing *Foxf1* expression in E8.5-E12.5 mouse embryos. (A,B). Early E8.5 embryos (six to eight pairs of somites), shown with (A) and without (B) yolk sac, express *Foxf1* in allantois, lateral mesoderm and posterior primitive streak. (C) Sections through E8.5 (six to eight pairs of somites) embryo show *Foxf1* expression in both splanchnic and somatic mesoderm at the hindgut level (top), but restricted to the splanchnic mesoderm at midgut (middle) and foregut (bottom) levels. (D) Early E8.5 conceptus (six to eight pairs of somites) with *Foxf1* expression in the blood islands seen as blue freckles on the yolk sac surface (right) and a conceptus hybridized with a sense control probe (left). (E,F) Dorsal (E) and ventral (F) views of E8.5 embryo (eight to ten pairs of somites) that has initiated turning show *Foxf1* expression in lateral mesoderm. (G) E9.5 embryo (14 to 18 pairs of somites) that has completed turning expresses *Foxf1* in splanchnic mesoderm. (H) *Foxf1* expression in the vasculature of E9.5 yolk sac (from embryo with 18-22 pairs of somites). (I,J) E10.5 embryos (35-40 pairs of somites) in aqueous solution (I) and clarified in aromatic alcohols (J) with *Foxf1* expression in sclerotomes, in mesenchyme lining the entire alimentary canal and in lung buds. (K) Close up ventral view of the dorsal midline at the lung bud level of E11.5 embryo (>45 pairs of somites) shows stripes of *Foxf1* expression through the center of each sclerotome. (L) Clarified E12.5 embryo with expression of *Foxf1* throughout the gastrointestinal tract, lungs and liver capsule. The stripes of *Foxf1* expression in sclerotomes gradually narrow as the vertebral chondrogenic mesenchyme differentiates in a cranio-caudal sequence. al, allantois; co, coelom; in, intestine; li, liver; lu, lung buds; oc, oral cavity; sc, sclerotome; so, somatic mesoderm; sp, splanchnic mesoderm; ys, yolk sac. Scale bars: 0.1 mm in C,H,K.

layer of the splanchnopleure (Fig. 1C). At E9.5, the yolk sac vasculature was well developed and *Foxf1* mRNA was found in the major blood vessels (Fig. 1H). *Foxf1* was not expressed in somites, but was turned on in sclerotomes, as they separated from the dermomyotome (Fig. 1J,K). Initially, *Foxf1* mRNA was found throughout the sclerotome, but as vertebral differentiation progressed in a cranio-caudal sequence, *Foxf1* was switched off in the chondrogenic mesenchyme at the junction of adjacent sclerotomes. It remained expressed in the central part of each sclerotome, in what will become the intervertebral disks (Fig. 1K,L; Mahlapuu et al., 1998). Splanchnic *Foxf1* expression persisted in mesenchyme surrounding the entire primitive gut (Fig. 1G,J,L) and in organs derived from it, such as lung buds and liver capsule (Fig. 1J,L; Mahlapuu et al., 1998). The allantoic expression was retained in the blood vessels of the umbilical cord.

Targeting the *Foxf1* locus

A *Foxf1* null allele was generated by homologous recombination (Fig. 2) in two ES cell lines (E14 and RW4), derived from different inbred mouse strains (129/Ola and 129/Sv). Chimeras generated with targeted cell clones derived from both E14 and RW4 cell lines passed the targeted allele through germ line when mated with CD1 and C57Bl/6 females. The mutation has been maintained on mixed 129/Ola-C57Bl/6, 129/Ola-CD1 and 129/Sv-C57Bl/6 backgrounds and *Foxf1*$^{-/-}$ embryos from all the different backgrounds have been examined and show identical phenotypes with 100% penetrance.

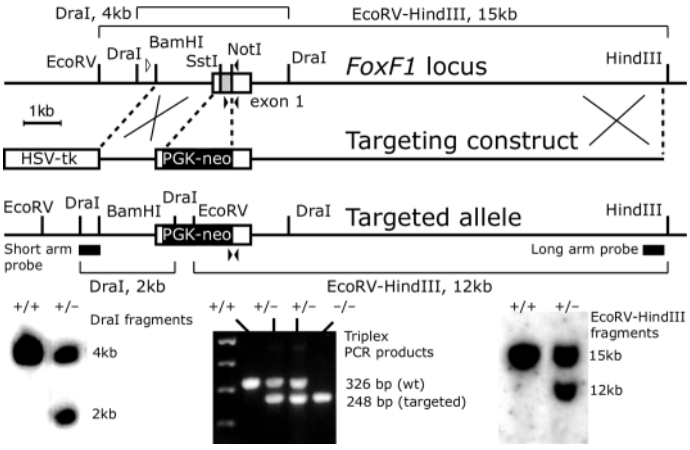

Fig. 2. Targeting the *Foxf1* gene. A PGK-neo cassette replaces the forkhead box (shaded area between *Sst*I and *Not*I) of *Foxf1* in the targeting construct containing a total of 12.5 kb of the *Foxf1* locus. G-418 and ganciclovir double resistant colonies obtained by electroporation of the targeting construct into ES cell lines RW4 and E14 were screened by PCR with a sense primer located upstream of the short arm (white arrowhead) and an antisense primer located 3′ of the *Not*I site in exon 1 (black arrowhead in antisense orientation). Homologous recombination was confirmed by Southern blotting of *Dra*I digested DNA hybridized with a probe (*Dra*I-*Bam*HI) located outside of the short arm and by double digestion with *Eco*RV and *Hin*dIII followed by hybridization with a probe from within the long arm. Both the *Eco*RV and *Hin*dIII sites in the *Foxf1* locus used for mapping are located outside of the targeting construct. For routine genotyping a triplex PCR was used with a common antisense primer located in the residual part of exon 1 (same as used for screening), a sense primer specific for the targeted allele in the PGK promoter and a wild-type-specific sense primer in the forkhead box of *Foxf1* (all designated by black arrowheads).

Foxf1 null embryos die at midgestation

No *Foxf1*$^{-/-}$ embryos survived beyond E10, but the Mendelian genotype frequencies observed in embryos analyzed at E8.5 and E9.5 (25.7% +/+; 51.1% +/–; 23.2% –/–; *n*=268) indicated that mutant mortality was not elevated before this stage. Up until approx. E8, or the appearance of the first pairs of somites, the mutant embryos were indistinguishable from their wild-type littermates and the first morphological and histological abnormalities were visible around E8.5, when the wild-type embryos have five to seven pairs of somites. The deformation of the *Foxf1* null embryos then rapidly aggravated, at E9.5 they were contorted beyond recognition and by E10.5 all mutant embryos were resorbed.

The *Foxf1* mutation affected development of both embryonic and extra-embryonic structures. The amnion – normally a thin, expanded membrane that covers the dorsal side of the embryo (Fig. 3A) – was small, tight and restricted the growth of mutant embryos (Fig. 3B,D). Histological sections revealed that the mutant amnion was abnormally thick and consisted of multiple layers of rounded cells instead of the characteristic flattened bilayer (Fig. 4F,G).

A normal allantois elongated and its distal end fused with the chorion by the time the embryo has developed five to seven pairs of somites (Fig. 4A). It then attained the shape of a funnel and underwent extensive vascularization (Fig. 4B). The *Foxf1*$^{-/-}$ allantois grew in size, but retained a primitive, bud-like shape (Fig. 3B,D). It did not elongate and failed to make contact with the chorion (Fig. 4C).

By the time wild-type embryos initiated the turning sequence (eight to ten pairs of somites), *Foxf1*$^{-/-}$ embryos began to exhibit a distinct asymmetry; the anterior part developed normally, whereas the posterior part was retarded and produced fewer somites. For example, the *Foxf1*$^{-/-}$ embryo shown in Fig. 3D has nine pairs of somites, but the development of its anterior part – cephalic neural fold, branchial arches, otic and optic vesicles – was similar to that of its wild-type littermates, which have 14-16 pairs of somites (Fig. 3C). The turning sequence is normally initiated at E8.5 and completed by E9.5. *Foxf1*$^{-/-}$ embryos, however, remained locked in the primitive position with the ventral side facing out and showed no tendency to turn (Fig. 3B,D). As a consequence, the midgut never formed. Somites appeared normal at the early stages, but later they became asymmetrically arranged on either side of an undulated neural tube (Fig. 3E), presumably caused by inability of the embryo to expand along the anteroposterior axis because of the constraints of the amnion. The growing head was either deformed inside the constricted amnion (Fig. 3B), or broke through it into the exocoelomic cavity (Fig. 3D).

Foxf1 is required for yolk sac vasculogenesis

At E9.5, *Foxf1* mutant embryos were severely disfigured, their yolk sacs were wrinkled, shrunken, anemic and lacked vasculature (Fig. 3F-K). Formation of the yolk-sac blood vessels begins with fusion of the blood islands into a primitive vascular plexus. At E8.5 this could be visualized as a honeycomb pattern formed by nucleated red blood cells expressing ζ-globin (*Hba-x*; Fig. 5A). In sections, the

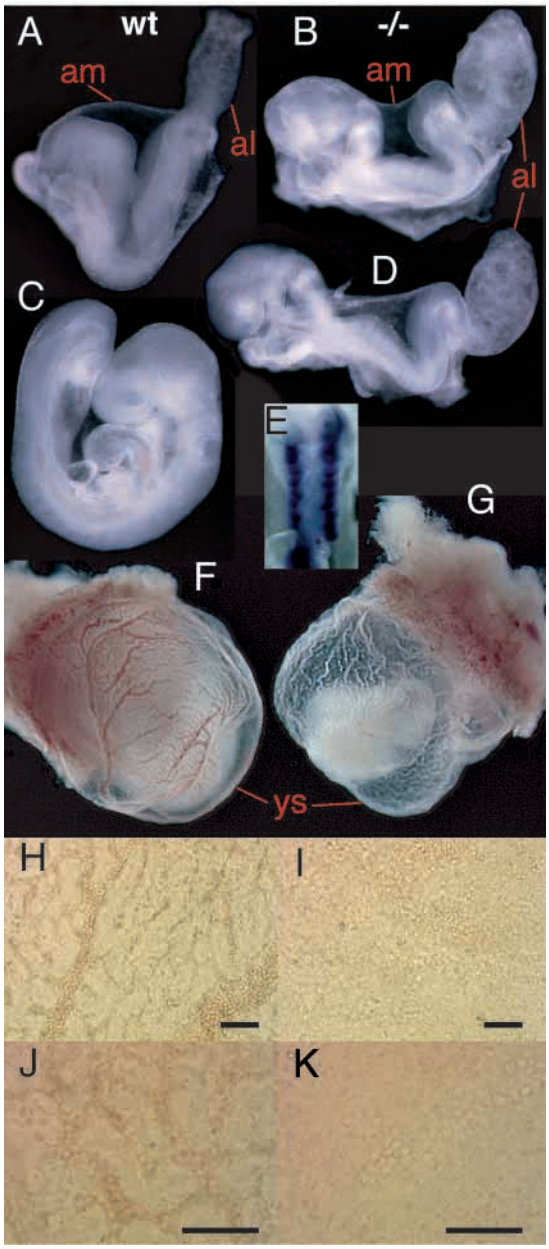

Fig. 3. Phenotype of *Foxf1* null embryos. (A) Early E8.5 wild-type embryo (six to eight pairs of somites) still in primitive (not turned) position with the distal end of the allantois uneven from the torn chorioallantoic fusion. (B-D) Two *Foxf1*$^{-/-}$, E8.5 embryos (B,D) compared with a wild type (+/+ or +/–) littermate (C), which has completed the turning sequence (advanced E8.5; 14-16 pairs of somites). The anterior part of the *Foxf1* null embryos (B,D) are at a developmental stage that corresponds to its wild-type littermates with visible otic and optic vesicles, branchial arches and closure of the neural tube at the hindbrain level. The posterior part of the null embryos is retarded compared with the anterior and has eight to nine pairs of somites. The mutant embryos (B,D) do not initiate the turning sequence, their allantois is swollen, bud-like and has not made contact with the chorion. Growth of the null embryos is constrained by the small and inflexible amnion; the head is either distorted inside it (B), or breaks through it into the exocoelomic cavity (D). (E) Dorsal view of a *Foxf1*$^{-/-}$, E8.5 embryo at a developmental stage similar to those shown in B,D. The somites (visualized by whole mount in situ hybridization with a *Meox1* probe) are seen asymmetrically arranged on either side of the zigzag shaped neural tube. (F-K) At E9.5 (18-22 pairs of somites in wild-type embryos) *Foxf1* null embryos (G,I,K) are severely disfigured inside the tight amnion and lack the vitelline vasculature characteristic of wild-type yolk sacs (F,H,J). al, allantois; am, amnion; ys, yolk sac. Scale bars: 0.1 mm in H-K.

hematopoietic cells were seen enclosed in blood vessels separated from the exocoelom by thin endothelial cells (Fig. 4D,J,L). In *Foxf1*-deficient yolk sacs no vascular plexus formed (Figs 4E,K,M, Fig. 5B). To investigate if the lack of vascularization was due to a differentiation defect in vascular precursor cells, we examined the expression of markers for the two dominating cell types in yolk sac blood vessels, endothelial cells and vascular smooth muscle cells. Platelet/endothelial cell adhesion molecule (Pecam) was present on endothelial cells of both yolk sac and embryo proper (Fig. 5G) and the gene for vascular smooth muscle α-actin (*Actvs*) was expressed in the smooth muscle cells that surround the major vessels (Fig. 5C,E). In the yolk sac mesoderm of *Foxf1* mutants both markers were expressed at a high level, which shows that differentiation of vascular cell types has been initiated (Fig. 5D,F,H). Hematopoietic cells also developed and could be identified by the expression of *Hba-x*, but were confined to large aggregates associated with the endoderm along the mesometrial border of the yolk sac (Fig. 5B). TGFβ1, which is produced by hematopoietic and endothelial cells (Akhurst et al., 1990), exhibited a change in expression pattern – from distributed throughout the yolk sac in wild type (Fig. 5I) to restricted to the mesometrial pole in *Foxf1* mutants (Fig. 5J) – which correlates with the aberrant distribution of hematopoietic cells.

VEGF and endothelial tyrosine kinase receptors are involved in various steps in yolk sac vascularization; inactivation of any of the genes encoding these proteins results in defect vasculogenesis, angiogenesis, or both (Neufeld et al., 1999). To investigate if the lack of vasculogenesis in *Foxf1* null yolk sacs was due to abrogation of this pathway, we compared the expression of *Flk1*, *Flt1*, *Flt4*, *Tie2* (*Tek* – Mouse Genome Informatics) and *Vegf* in +/– and –/– concepti using RT-PCR. As shown in Fig. 6, the expression levels of these genes in *Foxf1*$^{-/-}$ concepti did not differ from those in heterozygotes sufficiently to explain the total lack of vasculogenesis observed in the homozygote.

For the ligand to reach its receptor, VEGF signaling in the yolk sac requires an intimate contact between endodermal and mesodermal layers, and mutations that obstruct this association interfere with vasculogenesis (Dickson et al., 1995; George et al., 1993; Goumans et al., 1999; Oshima et al., 1996; Yang et al., 1993). In *Foxf1* mutants, however, endodermal and mesodermal layers of the yolk sac separated from each other. The poor connection was first evident at E8.5 (Fig. 4C,E) and at E9.5 only occasional points of attachment between mesoderm and endoderm remained (Fig. 4I,K,M). The disintegration of the yolk sac suggests defects in cell adhesion, but several observations indicated that altered intramesodermal cohesion rather than endodermal-mesodermal interaction is involved. First, factors known to be important for endodermal-mesodermal connection, such as fibronectin deposition (George et al., 1993), expression of α_5-integrin (Yang et al., 1993) and all the cadherins examined (E, N and VE, Carmeliet

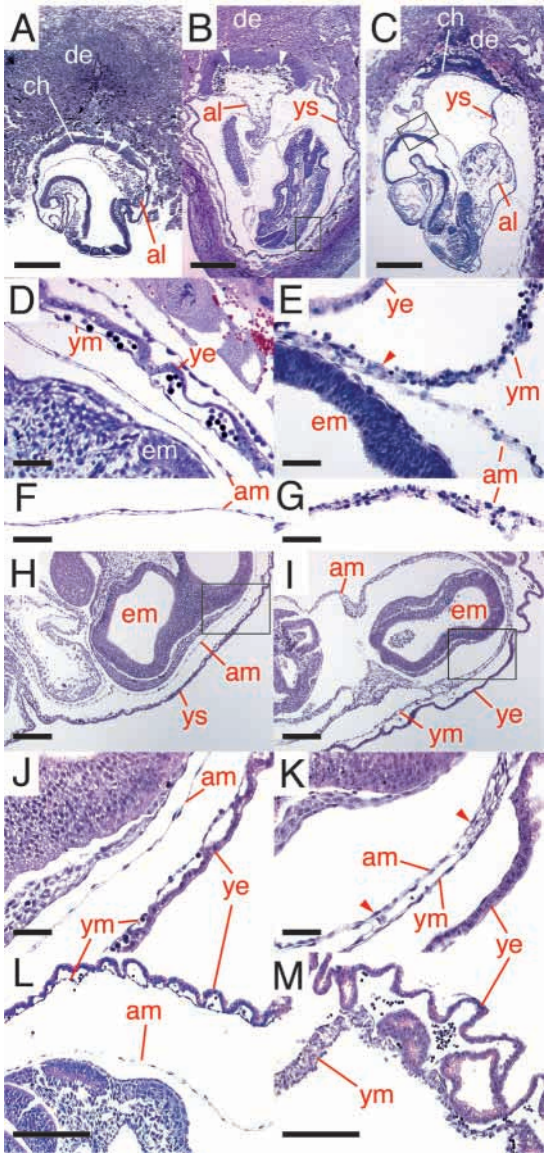

Fig. 4. Inactivation of *Foxf1* leads to defects in extra-embryonic mesoderm. (A) Sagittal section through early E8.5 (six pairs of somites) wild-type embryo. The distal end of the allantois has fused with the chorion (white arrowheads). (B) Intermediate E8.5 (10-12 pairs of somites) wild-type embryo with longitudinal section through the allantois showing the funnel shape and the extensive contact area between allantois and chorion (white arrowheads). (C) Sagittal section through E8.5 *Foxf1* null embryo at the same developmental stage as the wild-type embryo in B. The allantois is dense, bud-like and has not expanded to make contact with the chorion. (D) Close up view of the area boxed in B (wild-type embryo) showing vascularization of the yolk sac with blood vessels containing embryonic red blood cells and separated from the exocoelomic cavity by a thin layer of yolk sac mesoderm. Also note the thin, smooth appearance of the amnion. (E) Close up view of the area boxed in C (*Foxf1*$^{-/-}$ embryo) showing lack of yolk sac blood vessels, beginning separation between the endodermal and mesodermal layers of the yolk sac, thickening of the amnion and adherence between the mesodermal layers of amnion and yolk sac (red arrowhead). (F) Close up view of amnion of the wild-type embryo shown in B. (G) Close up view of amnion of the mutant embryo shown in C. (H) Section through E9.5 (18-22 pairs of somites) wild-type embryo enclosed in amnion and yolk sac. (I) Section through E9.5 *Foxf1* null embryo (littermate of the embryo in H), showing extensive separation of yolk sac mesoderm from the endoderm, thickening of the amnion and fusion between yolk sac mesoderm and amnion. (J) Close up view of the area boxed in H (wild-type embryo). (K) Close up view of the area boxed in I (*Foxf1*$^{-/-}$ embryo). Red arrowheads indicate points of adherence between amnion and yolk sac mesoderm. (L) Section through E9.5 (18-22 pairs of somites) wild-type embryo enclosed in amnion and yolk sac. (M) Section through E9.5 *Foxf1*$^{-/-}$ yolk sac (littermate of the embryo in L), showing thickening of the yolk sac mesoderm and how failure of the mesoderm to expand forces the yolk sac endoderm to fold in and out between the remaining points of attachment. al, allantois; am, amnion; ch, chorion; de, decidua; em, embryo; ye, yolk sac endoderm; ym, yolk sac mesoderm; ys, yolk sac. Scale bars: 0.5 mm in A-C; 0.05 mm in D-G,J,K; 0.2 mm in H,I; 0.1 mm in L,M.

et al., 1999; Radice et al., 1997), appeared unaffected by *Foxf1* deficiency, as judged by immunohistochemistry (data not shown). Secondly, although the bulk of the mesoderm detaches from the endoderm (Fig. 4C,E,I,K,M), the interface between mesodermal and endodermal cells seemed to be intact, since the inner surface of the endoderm was lined by Pecam-positive mesodermal cells (Fig. 5H). A driving force behind the separation appeared to be an inability of the mesoderm to expand along with the endoderm as the embryo grew, leaving the mesodermal layer abnormally thick and constricted around the embryo (Fig. 4C,E,I,K,M).

Foxf1 is required for differentiation of allantois and amnion

Defect mesodermal expansion, accompanied by lack of vascularization, also characterizes the *Foxf1*$^{-/-}$ allantois. The vasculogenesis defect in the mutant allantois may be explained by altered expression of the VEGF receptor Flk1. Normally the entire allantois expresses *Flk1* (Fig. 5M), but in *Foxf1*$^{-/-}$ allantois the expression was reduced and confined to the base (Fig. 5N). Since vasculogenesis is initiated in the distal part of the allantois (Downs et al., 1998), its absence in *Foxf1* mutants is consistent with the lack of Flk1 in this region. Two other markers for allantoic differentiation, *Tgfb1* and the T-box transcription factor *Tbx2*, exhibit a similar change of expression pattern as a result of *Foxf1* deficiency. mRNA for both genes is normally present in the whole allantois (Fig. 5I,K), but was found only at the base in *Foxf1* mutants (Fig. 5J,L). The paracrine protein BMP4 is involved in several aspects of mesoderm formation and specification, including allantoic differentiation (Lawson et al., 1999; Winnier et al., 1995). In *Foxf1* null allantois the expression of *Bmp4* was lost (Fig. 5O,P), which is likely to contribute to the observed defects in allantoic development.

The amnion of *Foxf1*-deficient concepti was thick, inflexible and did not expand to accommodate the growing embryo. Misexpression in the amnion of several genes normally associated with vasculogenesis indicates fundamental errors in differentiation of *Foxf1*$^{-/-}$ amniotic mesoderm. It expressed *Actvs* (Fig. 5F), normally associated with major blood vessels (Fig. 5C,E), and it was immunoreactive for Pecam (Fig. 5H), which is a cell surface marker for endothelial cells of yolk sac and embryo proper. The *Foxf1*-deficient amnion was also a site for ectopic hematopoiesis. Nucleated red blood cells, identified by *Hba-x* expression, could be seen budding off from the outer

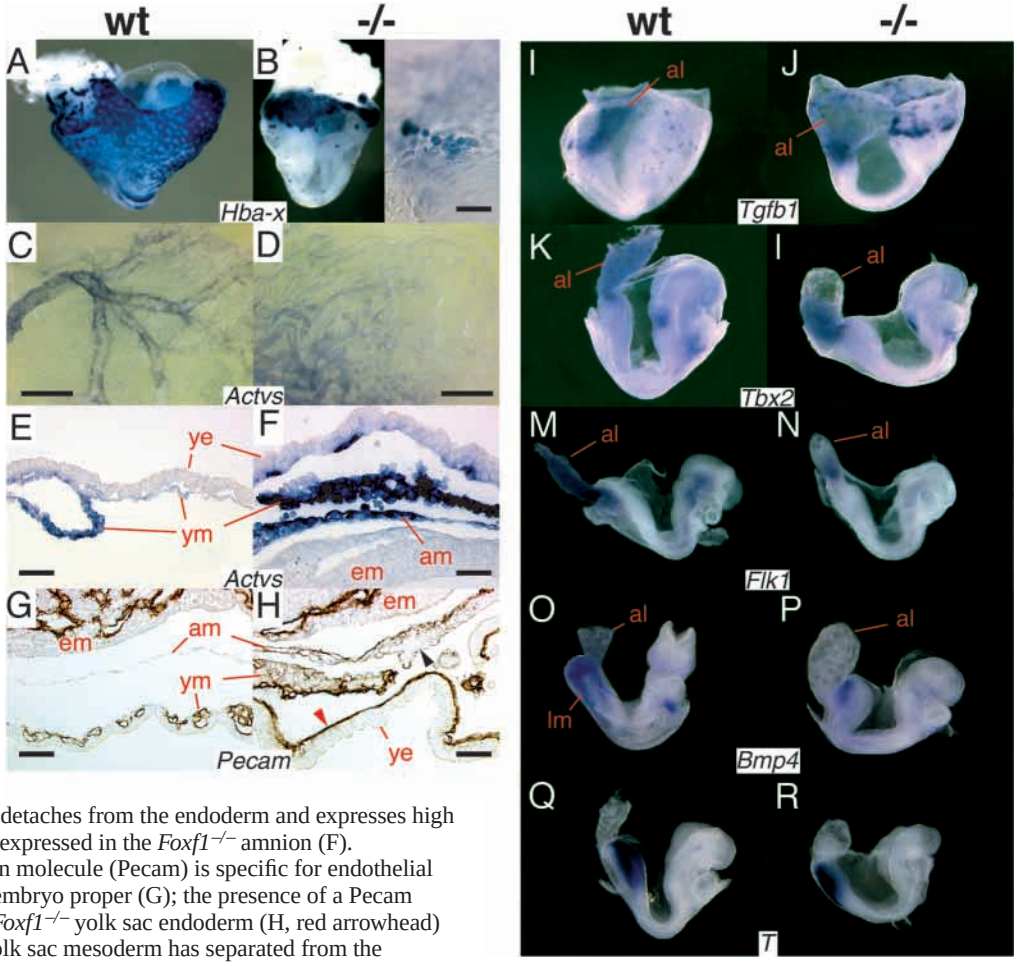

Fig. 5. Defect differentiation of embryonic and extra-embryonic mesoderm in response to inactivation of *Foxf1* is revealed by altered expression patterns of differentiation markers. Analysis of E8.5 (six to ten pairs of somites; A,B,I-R) and E9.5 (18–22 pairs of somites; C-H) wild-type (A,C,E,G,I,K,M,O,Q) and *Foxf1*-deficient (B,D,F,H,J,L,N,P,R) concepti by in situ hybridization (A-F,I-R) and immunohistochemistry (G,H). (A,B) *Hba-x* (ζ-globin) expression identifies embryonic red blood cells which fill the vascular plexus in wild-type yolk sacs (A), but are aggregated in the mesometrial pole of *Foxf1*-deficient yolk sacs (B, left). The right panel in B shows *Hba-x* expressing, hematopoietic cells budding off from the surface of the amnion in a *Foxf1*$^{-/-}$ conceptus. (C-F) Vascular smooth muscle α-actin (*Actvs*) expression identifies the smooth muscle cells of the major blood vessels of an E9.5 yolk sac (C,E); the yolk sac mesoderm of *Foxf1*-deficient concepti detaches from the endoderm and expresses high levels of *Actvs* (D,F). *Actvs* is also misexpressed in the *Foxf1*$^{-/-}$ amnion (F). (G,H) Platelet/endothelial cell adhesion molecule (Pecam) is specific for endothelial cells of blood vessels in yolk sac and embryo proper (G); the presence of a Pecam positive lining of the inner surface of *Foxf1*$^{-/-}$ yolk sac endoderm (H, red arrowhead) shows that, although the bulk of the yolk sac mesoderm has separated from the endoderm, a thin layer of mesodermally derived cells of the endothelial lineage remains firmly associated with the endoderm. (H) In *Foxf1*-deficient concepti Pecam is also expressed in the undifferentiated yolk sac mesoderm and misexpressed in the amnion. Note the fusion between the detached yolk sac mesoderm and the amnion (H, black arrowhead). (I,J) *Tgfb1* expression in the yolk sac matches the distribution of hematopoiesis and is found throughout the wild-type yolk sac (I, faint blue spots), but is confined to its mesometrial pole in *Foxf1* mutants (J). *Tgfb1* expression is also found in the entire wild-type allantois (I), but only in the basal part of the *Foxf1*$^{-/-}$ allantois (J). (K-N) Two additional markers for allantoic differentiation that are normally expressed throughout the allantois, *Tbx2* (K) and *Flk1* (M), exhibit similar changes in expression in response to *Foxf1* deficiency as *Tgfb1*. In the *Foxf1* mutant, expression of both *Tbx2* and *Flk1* is missing from the distal allantois and is instead restricted to the base of allantois, adjacent to the posterior primitive streak (L,N). (O,P) In the posterior part of the embryo, *Bmp4* is expressed in the posterior primitive streak, in lateral mesoderm and in extra-embryonic mesoderm, including allantois (O; Winnier et al., 1995); in *Foxf1*$^{-/-}$ concepti there is no *Bmp4* expression in the allantois and in the posterior part of the embryo proper, including the lateral mesoderm, the expression is much weaker than normal (P). Only in the primitive streak region is there still moderate expression of *Bmp4*. (Q,R) Expression of *T* (*Brachyury*) identifies undifferentiated mesoderm of the primitive streak region and shows that less of this mesoderm is present in the *Foxf1* mutant (R) compared with the wild-type embryo (Q). al, allantois; am, amnion; em, embryo; lm, lateral mesoderm; ye, yolk sac endoderm; ym, yolk sac mesoderm. Scale bars: 0.05 mm in B,E-H; 0.5 mm in C,D.

surface of the amnion (Fig. 5B). In gene expression profile, the *Foxf1*$^{-/-}$ amniotic mesoderm thus resembles yolk sac mesoderm. Altered cell adhesion properties support this notion; the mesodermal layers of amnion and yolk sac frequently adhered to each other in *Foxf1* mutants (Fig. 4C,E,I,K) and as the yolk sac mesoderm separated from the endoderm, it occasionally fused with the amnion (Fig. 5H).

Inactivation of *Foxf1* leads to misexpression of *Vcam1*

The abnormal adhesion between distinct types of extra-embryonic mesoderm, the thickness and inability to expand of both yolk sac and amniotic mesoderm, and the failure of the allantois to reshape in *Foxf1* mutants all suggest altered expression of cell adhesion proteins. Vascular cell adhesion molecule 1 (VCAM1) mediates adherence between different cellular populations by binding to α_4-integrin on the target cells (Elices et al., 1990). During embryonic development, *Vcam1* is expressed in the peripheral cells of the allantois (Fig. 7A,C) and is responsible for the chorioallantoic fusion together with α_4-integrin in the chorion (Gurtner et al., 1995; Kwee et al., 1995; Yang et al., 1995). It is also found in the yolk sac endoderm (Fig. 7A,E,G) where it may interact with α_4-integrin in the mesodermal layer. Inactivation of *Foxf1* results in a dramatic expansion in the expression range of *Vcam1* in extra-embryonic mesoderm. In *Foxf1* mutants VCAM1 was found in amnion (Fig. 7H), in yolk sac mesoderm (Fig. 7B,F) and throughout the allantois (Fig. 7B,D).

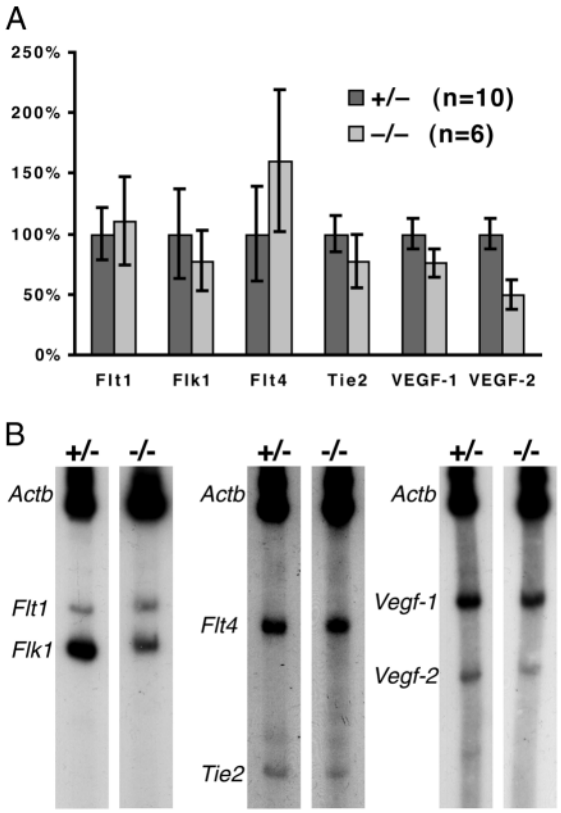

Fig. 6. The vascularization defect in *Foxf1*$^{-/-}$ yolk sacs cannot be explained by lack of expression of vasculogenic or angiogenic tyrosine kinase receptors or growth factors. (A) mRNA from individual E8.5 concepti was analyzed by RT-PCR. The expression level of each gene was estimated from the ratio between the cognate PCR product and a β-actin (*Actb*) internal control at three time points during the PCR program. Averages from the analysis of ten +/– and six –/– concepti are shown. VEGF1 and VEGF2 refer to alternatively spliced variants of *Vegf* mRNA. Error bars represent s.e.m. (B) Representative autoradiograms from the data on which the diagram in A was based.

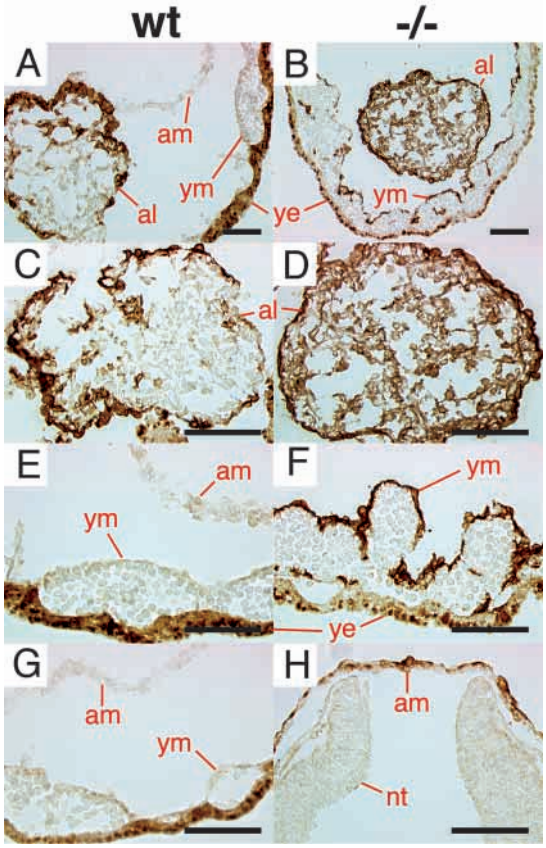

Fig. 7. Foxf1 is essential for restriction of the expression range of *Vcam1* in extra-embryonic mesoderm. (A-H) Immunostainings with anti-VCAM1 on transversal sections through the mesometrial end of E8.5 (six to eight pairs of somites) concepti. VCAM1 is normally found in the yolk sac endoderm (A,E,G) and in the peripheral cells of the allantois (A,C), but not in the internal vasculogenic mesenchyme of the allantois (A,C) or in mesoderm of yolk sac and amnion (A,E,G). *Foxf1*-deficient concepti express *Vcam1* in all extra-embryonic mesoderm: amniotic (H), yolk sac (B,F) and all allantoic (B,D). Only the masses of hematopoietic cells, characteristic of the mesometrial pole of *Foxf1*$^{-/-}$ yolk sacs, are VCAM1 negative (B,F). Scale bars: 0.1 mm. al, allantosis; am, amnion; nt, neural tube; ye yolk sac endoderm; ym, yolk sac mesoderm.

Foxf1 is involved in lateral plate differentiation and coelom formation

Up until the developmental stage at which *Foxf1*$^{-/-}$ embryos die, the only sites of *Foxf1* expression in wild-type embryo proper are in mesoderm of the posterior primitive streak and lateral plate. During this phase, the dichotomy of the lateral mesoderm takes place, accompanied by a narrowing of the lateral *Foxf1* expression range to encompass splanchnic mesoderm only. To investigate if *Foxf1* is involved in differentiation of the lateral plate, we examined the division of somatopleure and splanchnopleure. This subdivision of the lateral plate, which creates the coelomic cavity (Fig. 8A,C,E,G), was disturbed in mutants (Fig. 8B,D,F,H). In some *Foxf1*-deficient embryos the somatic and splanchnic layers remained fused (Fig. 8D,F,H). In the cases where a cavity was formed, the separation was often incomplete and interrupted by residual points of attachment. This gives the edges of the coelom a torn appearance (Fig. 8B,D), quite distinct from the organized, epithelial-like cells that line a normal coelom (Fig. 8A,C,E,G). Formation of the involuted hindgut diverticulum (Fig. 8A,I) was also delayed in the mutant and instead the posterior visceral endoderm was flat and enclosed in a wide yolk-sac pocket (Fig. 8B,J).

A marker for differentiation of the lateral plate is expression of the homeobox gene *Irx3* in mesoderm of somatopleure (Fig. 8I,K, Bellefroid et al., 1998; Bosse et al., 1997; Funayama et al., 1999). Activation of *Irx3* in somatic mesoderm coincided with *Foxf1* being switched off in this layer (Fig. 1D). In *Foxf1* null embryos, however, the range of *Irx3* expression was extended to the entire lateral mesoderm, including that of the splanchnopleure (Fig. 8L).

Foxf1 promotes mesodermal proliferation

The posterior part of *Foxf1* null embryos appeared developmentally retarded compared with the anterior part, which developed on a par with wild-type littermates (Fig. 3B-D). The caudal end of mutant embryos was thin and somite formation slow, a phenotype consistent with paucity of

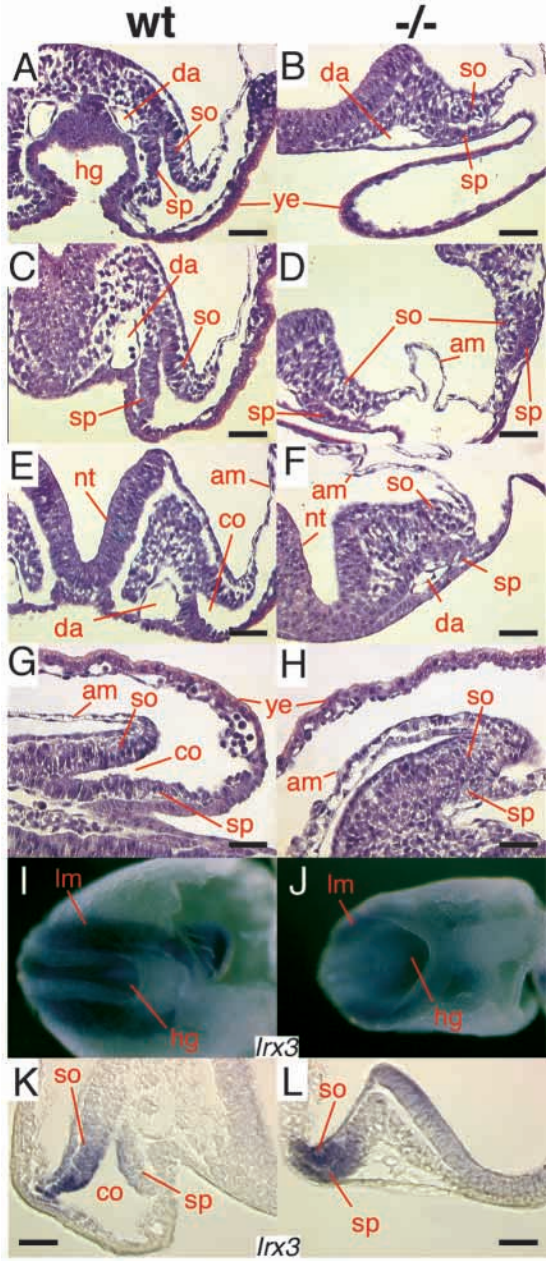

Fig. 8. Foxf1 is involved in lateral plate differentiation and coelom formation. (A-H) Sections of early E8.5 (six to eight pairs of somites) wild-type (A,C,E,G) and *Foxf1*$^{-/-}$ (B,D,F,H) embryos. Differentiation of the lateral plate into somatopleure and splanchnopleure and the associated formation of a coelomic cavity is disturbed in *Foxf1*$^{-/-}$ embryos. Separation of the somatic and splanchnic mesodermal layers is incomplete and the coelomic cavity is either missing or interrupted by residual points of adherence. The formation of a hindgut diverticulum (A) is delayed in *Foxf1* null embryos and a yolk sac fold instead covers the flat endoderm (B; see also I,J). (I-L) Whole-mount in situ hybridization of E8.5 (six to eight pairs of somites) wild-type (I,K) and *Foxf1*$^{-/-}$ (J,L) concepti with a probe for iroquois-related homeobox 3 (*Irx3*). *Irx3* is expressed in the lateral plate mesoderm (I,J) and sections (K,L) show that in wild type it is confined to the somatopleure (K). In *Foxf1* null embryos *Irx3* is expressed throughout the lateral plate, including the splanchnopleure (L). am, amnion; co, coelomic cavity; da, dorsal aorta; hg, hindgut diverticulum; lm, lateral mesoderm; nt, neural tube; so, somatic mesoderm; sp, splanchnic mesoderm; ye, yolk sac endoderm. Scale bars: 0.05 mm in A-H,K,L.

embryonic mesoderm. This interpretation is supported by the expression pattern of *T* (*Brachyury*), which identifies undifferentiated mesoderm generated in the primitive streak. The expression level of *T* in *Foxf1* mutants was comparable with that in wild-type embryos, but the amount of *T*-expressing mesoderm was substantially lower (Fig. 5Q,R). Paucity of mesoderm could result either from poor survival, or a lower proliferation rate of mesodermal cells. To investigate these possibilities, we analyzed apoptosis in E8.5 embryos at the stage when morphological differences are first visible. Scattered apoptotic cells were detected in both *Foxf1*-deficient and wild-type embryos, but the majority of these were of endodermal or neuroectodermal origin (Fig. 9A,B). Very few embryonic mesodermal cells stained positive in the TUNEL assay and the frequency was not elevated in the mutant. Neither was cell death in extra-embryonic mesoderm of amnion, yolk sac or allantois more common in the *Foxf1* mutant. Hence, we can rule out mesoderm depletion caused by inferior survival as a mechanism behind the *Foxf1* mutant phenotype.

BrdU incorporation was used to measure the proliferation rate of different cell populations and to compare the levels in normal and *Foxf1*$^{-/-}$ concepti. In mesoderm of the posterior primitive streak the frequency of replicating cells was significantly lower in *Foxf1* mutants than in wild-type littermates (Fig. 9I,J,M). This was not due to a generally lower growth rate in the mutant, since the frequency of BrdU-positive nuclei in neuroectoderm did not differ, either in the anterior part of the embryos (Fig. 9K,L) or at the primitive streak level (Fig. 9I,J,M). The slow growth and mesoderm deprivation of the posterior part of *Foxf1*-deficient embryos thus appear to be consequences of a reduced production of mesodermal cells in the posterior primitive streak. BMP4 is a positive regulator of mesodermal proliferation in this region and *Bmp4* null embryos that survive to this stage have a paucity of posterior mesoderm, much like the *Foxf1* mutants (Winnier et al., 1995). We therefore investigated the expression of *Bmp4* in *Foxf1* null embryos and found that the level of *Bmp4* mRNA was significantly reduced, both in the posterior primitive streak and lateral plate (Fig. 5O,P). This decrease in BMP4 signaling, caused by lack of *Foxf1* activity, may be responsible for the lower mesodermal proliferation rate.

The abnormal histology of *Foxf1*$^{-/-}$ extra-embryonic mesoderm makes quantitative comparisons of BrdU incorporation difficult when it comes to amnion, yolk sac and allantois. However, it is clear that there is a high proliferation rate in extra-embryonic mesoderm of *Foxf1* mutants and that the failure to expand observed both in amnion, yolk sac mesoderm and allantois cannot be explained by a lack of cell division (Fig. 9C-H). The growth in thickness (amnion and yolk sac mesoderm) or size (allantois) of mutant extra-embryonic structures supports this conclusion.

DISCUSSION

Foxf1 null embryos develop normally up until the early somite stage, but die halfway through gestation owing to multiple

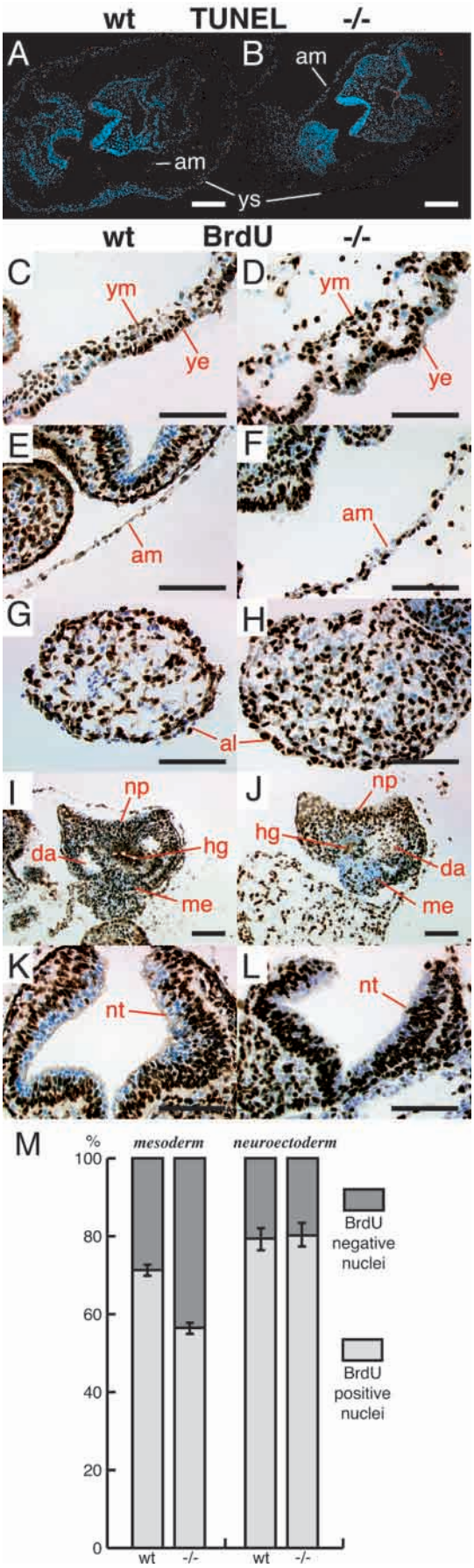

Fig. 9. Apoptosis and proliferation assays. (A,B) TUNEL assay on transversal section of E8.5 (eight to ten pairs of somites) embryos enclosed in amnion and yolk sac. Scattered apoptotic cells (red Cy3 staining on background of blue DAPI counterstain) are seen in both wild-type (A) and mutant (B), most of which are located in neuroectoderm and endodermal epithelia. The assay does not reveal any signs of increased cell death in *Foxf1*$^{-/-}$ embryonic or extra-embryonic mesoderm. (C,L) Cell proliferation in E8.5 (9-11 pairs of somites) concepti measured by BrdU incorporation (brown nuclear staining against background of blue nuclear counterstain). (C-H) The rates of cell proliferation in extra-embryonic mesoderm of yolk sac (C,D), amnion (E,F) and allantois (G,H) are comparable between wild type (C,E,G) and mutant (D,F,H). (I,J) Transversal sections through the caudal end of wild type (I) and mutant (J) embryos at the primitive streak level show a lower rate of mesodermal proliferation in the Foxf1 mutant, but equivalent rates in neural plate. (K,L) Cells in the neural tube have the same proliferation rates in mutant (L) and wild type (K). (M) Frequencies of BrdU-positive nuclei in mesoderm and neuroectoderm of wild type and *Foxf1*$^{-/-}$ E8.5 embryos at the primitive streak level (averages±s.e.m.). Mesodermal nuclei were counted on 14 sections (4725 nuclei in total) derived from eight embryos (four wild type and four null) and neuroectodermal nuclei on eight sections from the same embryos. The difference in proliferation rate between wild-type and mutant mesoderm is statistically significant (P=2.7×10^{-5} in a two-tailed t-test). al, allantois; am, amnion; da, dorsal aorta; hg, caudal extremity of hindgut diverticulum; me, mesoderm of primitive streak region; np, neural plate; nt, neural tube; ye, yolk sac endoderm; ym, yolk sac mesoderm; ys, yolk sac. Scale bars: 0.2 mm in A,B; 0.1 mm in C-L.

defects in extra-embryonic structures. The amnion constrains and deforms the growing embryo and the absence of a yolk-sac vasculature deprives it of a way to exchange metabolites with the mother. No placentation occurs, owing to the lack of chorioallantoic fusion, and by E10 extensive necrosis commences, presumably caused by hypoxia.

Histological analysis show that the defects reside in the extra-embryonic mesoderm, which is also where *Foxf1* normally is expressed. The frequency of apoptotic mesodermal cells is not elevated and a role for *Foxf1* in survival of this cell population can thus be excluded as the cause of the mutant phenotype. The shrunken appearance of extra-embryonic structures suggested that mesodermal proliferation might be compromised, but two observations argue against this. First, BrdU incorporation reveals a high frequency of replicating cells in extra-embryonic mesoderm. Second, the lack of expansion in the affected structures is replaced by a growth in thickness. Instead, both the histology and the altered expression patterns of several diagnostic genes indicate that *Foxf1* is an essential regulator of extra-embryonic mesoderm differentiation. In the absence of Foxf1 the amnion displays properties normally confined to the yolk sac, such as expression of markers for vascular smooth muscle cells, for the endothelial lineage and those indicating ectopic hematopoiesis. Misexpression of *Vcam1* is seen in amnion, in yolk sac mesoderm and internally in allantois. Mutant allantois lacks expression of *Bmp4* and – in the distal part – *Tgfb1*, *Flk1* and *Tbx2*, all of which are associated with normal allantoic development.

Foxf1$^{-/-}$ concepti do not form the chorioallantoic fusion, which is essential for placentation. This process is also inhibited by disruption of *Vcam1* or *Itga4* (α_4-integrin) (Gurtner et al., 1995; Kwee et al., 1995; Yang et al., 1995). In *Foxf1* mutants the allantois expresses *Vcam1* and it is possible

that fusion would take place if contact with the chorion was made. The size and appearance of the *Foxf1*-deficient allantois indicate that its inability to expand and reach the chorion is the limiting factor. Blood vessel formation in allantois is initiated in its distal part (Downs et al., 1998) and the lack of *Flk1* expression at this site explains why no allantoic vasculogenesis occurs in *Foxf1* mutants.

Yolk sac vasculogenesis is a well-studied process and depends on the proper functioning of a number of factors. Signaling through VEGF receptors and related tyrosine kinase receptors is essential for differentiation of vascular cell types, but *Foxf1* does not appear to be required for expression of components in this signaling pathway. Another important factor is an intimate contact between the mesodermal and endodermal layers. It is therefore likely that their separation in *Foxf1*-deficient yolk sacs contribute to the failure of vasculogenesis. However, in contrast to other described mutants with endodermal-mesodermal dissociation, in which cell-matrix adhesion is impaired (George et al., 1993; Goumans et al., 1999; Yang et al., 1993), *Foxf1* mutants appear to have an intact connection between the two cell types. What looks like a separation between mesoderm and endoderm seems to be detachment of the bulk of the mesoderm from a thin layer of mesodermal cells attached to the endoderm. This interpretation is supported by normal fibronectin deposition, normal integrin expression and by the presence of a thin, continuous lining of Pecam-positive cells along the entire inner surface of the endoderm. The Pecam-positive cells may be the equivalent of the endothelial cells that separate the lumen of normal yolk sac blood vessels from the endoderm. The primary cell adhesion defect in *Foxf1* null yolk sacs thus seems to be in intramesodermal cohesion.

Yolk-sac hematopoiesis does not require *Foxf1*, but the area in which hematopoiesis occurs is altered from the entire yolk sac in wild-type to a zone along the border with the decidua in the mutant. Displacement of hematopoietic cells has also been observed in concepti lacking *Tgfb1* (Dickson et al., 1995) and inhibited TGFβ signaling as a result of disruption of *Tgfb1* or the type II TGFβ receptor (Oshima et al., 1996) affects yolk sac vascularization and integrity. This rises the possibility that *Foxf1* may participate in the generation or reception of TGFβ signaling. The altered expression pattern of *Tgfb1* in *Foxf1* null concepti supports the hypothesis that *Foxf1* is involved in regulation of *Tgfb1* expression in yolk sac and allantois.

Binding of VCAM1 to α_4-integrin mediates association between different cell populations and under normal circumstances VCAM1 and α_4-integrin are never co-expressed in the same cell. In the adult, cytokine-activated endothelial cells express VCAM1, which recruits lymphocytes through binding to their α_4-integrins (Elices et al., 1990). During embryonic development, the only site of VCAM1 expression in extra-embryonic mesoderm is in the peripheral cells of the allantois. α_4-integrin, on the other hand, is widely expressed in extra-embryonic mesoderm, including amnion and yolk sac (Ogawa et al., 1999). A consequence of misexpression of *Vcam1* in *Foxf1*$^{-/-}$ extra-embryonic mesoderm is therefore that receptor and ligand are present on the same cells. The defects in allantois, amnion and yolk sac that result from *Foxf1* deficiency all implicate altered cell adhesion properties with enhanced intramesodermal cohesion. The abnormal fusion between amniotic and yolk sac mesoderm also reveals an affinity between cell types that normally do not interact. This could be a direct effect of interactions between α_4-integrin and misexpressed VCAM1.

Little is known about the mechanisms that lead to coelom formation in the embryo proper, but signaling by both ectoderm and endoderm is required, and maintenance of somatic mesoderm depends on BMPs secreted by the ectoderm (Funayama et al., 1999). The homeobox gene *Irx3* is expressed in somatic mesoderm (Bellefroid et al., 1998; Bosse et al., 1997) in response to ectodermal signals (Funayama et al., 1999), whereas *Foxf1* becomes restricted to the splanchnic mesoderm. In *Foxf1*-deficient embryos, *Irx3* is expressed in the entire lateral plate mesoderm, including the splanchnic component, which suggests that *Irx3* expression in splanchnic mesoderm is normally inhibited by *Foxf1* and that these two transcription factors have antagonistic roles in the dichotomy of the lateral plate.

A lower proliferation rate of mesodermal cells in the posterior primitive streak leads to reduction in the amount of mesoderm in the embryo proper and explains the underdeveloped appearance of the posterior part of *Foxf1*$^{-/-}$ embryos. BMP4, which is expressed in the posterior primitive streak, is believed to be a mitogen for undifferentiated mesoderm (Winnier et al., 1995). *Bmp4* null embryos have a variable phenotype; most die around gastrulation (approx. E6.5), but on some genetic backgrounds a proportion of the mutant embryos survive until the early somite stage and show severe defects, particularly in the extra-embryonic mesoderm (Winnier et al., 1995). Occasional embryos even complete the turning sequence and develop up to 23 pairs of somites (Lawson et al., 1999). *Bmp4*$^{-/-}$ embryos that survive into the somite stage have defects very similar to those of *Foxf1* mutants, with paucity of mesoderm in the posterior part (Lawson et al., 1999; Winnier et al., 1995). The phenotypic resemblance, which may indicate a functional relation, is also seen in extra-embryonic mesoderm. *Bmp4* is essential for normal development of allantois and for yolk-sac vascularization (Lawson et al., 1999). The *Bmp4*-deficient yolk sac is reported to have a 'blebby' appearance, caused by separation of the endodermal and mesodermal layers (Winnier et al., 1995). The altered pattern and level of *Bmp4* expression in *Foxf1* mutants is compatible with activation of *Bmp4* by Foxf1. Foxf1 appears to contribute to *Bmp4* expression in the posterior part of the embryo proper and to be essential for its expression in allantois; a difference that may be related to the less severe *Foxf1*$^{-/-}$ phenotype in the embryo, compared with extra-embryonic structures. Further support for a connection between *Foxf1* and BMP signaling comes from the knockout of *Smad5* (*Madh5*; Chang et al., 1999), which encodes a signal transducer for BMPs (Heldin et al., 1997). *Smad5*-deficient concepti exhibit retarded growth of the allantois, poor expansion of the amnion and ectopic amniotic hematopoiesis.

A majority of *Bmp4* null embryos arrest already at the gastrulation stage with a block in mesoderm formation (Lawson et al., 1999; Winnier et al., 1995). Since all *Foxf1* mutants develop normally into the somite stage, it is clear that *Foxf1* is not required for mesodermal *Bmp4* expression during gastrulation. On the other hand, some *Bmp4*-deficient embryos, believed to be rescued by other BMPs and/or maternal BMP4, complete the turning sequence and apparently have no major defects in amnion growth. This demonstrates that the abnormalities in *Foxf1*$^{-/-}$ embryos, which show very little variability between individual concepti and are more severe in

extra-embryonic structures, cannot be explained solely by effects on *Bmp4* expression.

We thank Drs B. L. M. Hogan, B. G. Herrmann, T. Yamaguchi, J. M. Partanen and R. J. Bollag for gifts of plasmids; A. Linde and F. Eshi for technical advice; C. Betsholtz for E14 cells; and M. Hulander for teaching us morula aggregation. This work was funded by grants from The Swedish Cancer Foundation and The Assar Gabrielsson Foundation.

REFERENCES

Aitola, M., Carlsson, P., Mahlapuu, M., Enerbäck, S. and Pelto-Huikko, M. (2000). Forkhead transcription factor FoxF2 is expressed in mesodermal tissues involved in epithelio-mesenchymal interactions. *Dev. Dyn.* **18**, 136-149.

Akhurst, R. J., Lehnert, S. A., Faissner, A. and Duffie, E. (1990). TGF beta in murine morphogenetic processes: the early embryo and cardiogenesis. *Development* **108**, 645-656.

Bellefroid, E. J., Kobbe, A., Gruss, P., Pieler, T., Gurdon, J. B. and Papalopulu, N. (1998). Xiro3 encodes a Xenopus homolog of the Drosophila Iroquois genes and functions in neural specification. *EMBO J.* **17**, 191-203.

Blixt, Å., Mahlapuu, M., Aitola, M., Pelto-Huikko, M., Enerbäck, S. and Carlsson, P. (2000). A forkhead gene, *FoxE3*, is essential for lens epithelial proliferation and closure of the lens vesicle. *Genes Dev.* **14**, 245-254.

Bosse, A., Zülch, A., Becker, M. B., Torres, M., Gómez-Skarmeta, J. L., Modolell, J. and Gruss, P. (1997). Identification of the vertebrate Iroquois homeobox gene family with overlapping expression during early development of the nervous system. *Mech. Dev.* **69**, 169-181.

Carmeliet, P., Lampugnani, M. G., Moons, L., Breviario, F., Compernolle, V., Bono, F., Balconi, G., Spagnuolo, R., Oostuyse, B., Dewerchin, M. et al. (1999). Targeted deficiency or cytosolic truncation of the VE-cadherin gene in mice impairs VEGF-mediated endothelial survival and angiogenesis. *Cell* **98**, 147-157.

Chang, H., Huylebroeck, D., Verschueren, K., Guo, Q., Matzuk, M. M. and Zwijsen, A. (1999). Smad5 knockout mice die at mid-gestation due to multiple embryonic and extraembryonic defects. *Development* **126**, 1631-1642.

Chang, H. H., Schwartz, Z. and Kaufman, M. H. (1996). Limb and other postcranial skeletal defects induced by amniotic sac puncture in the mouse. *J. Anat.* **189**, 37-49.

Clevidence, D. E., Overdier, D. G., Peterson, R. S., Porcella, A., Ye, H., Paulson, K. E. and Costa, R. H. (1994). Members of the HNF-3/forkhead family of transcription factors exhibit distinct cellular expression patterns in lung and regulate the surfactant protein B promoter. *Dev. Biol.* **166**, 195-209.

Dickson, M. C., Martin, J. S., Cousins, F. M., Kulkarni, A. B., Karlsson, S. and Akhurst, R. J. (1995). Defective haematopoiesis and vasculogenesis in transforming growth factor-beta 1 knock out mice. *Development* **121**, 1845-1854.

Downs, K. M. (1998). The murine allantois. *Curr. Top. Dev. Biol.* **39**, 1-33.

Downs, K. M., Gifford, S., Blahnik, M. and Gardner, R. L. (1998). Vascularization in the murine allantois occurs by vasculogenesis without accompanying erythropoiesis. *Development* **125**, 4507-4520.

Elices, M. J., Osborn, L., Takada, Y., Crouse, C., Luhowskyj, S., Hemler, M. E. and Lobb, R. R. (1990). VCAM-1 on activated endothelium interacts with the leukocyte integrin VLA-4 at a site distinct from the VLA-4/fibronectin binding site. *Cell* **60**, 577-584.

Ferrara, N., Carver-Moore, K., Chen, H., Dowd, M., Lu, L., O'Shea, K. S., Powell-Braxton, L., Hillan, K. J. and Moore, M. W. (1996). Heterozygous embryonic lethality induced by targeted inactivation of the VEGF gene. *Nature* **380**, 439-442.

Fong, G. H., Rossant, J., Gertsenstein, M. and Breitman, M. L. (1995). Role of the Flt-1 receptor tyrosine kinase in regulating the assembly of vascular endothelium. *Nature* **376**, 66-70.

Fong, G. H., Zhang, L., Bryce, D. M. and Peng, J. (1999). Increased hemangioblast commitment, not vascular disorganization, is the primary defect in flt-1 knock-out mice. *Development* **126**, 3015-3025.

Funayama, N., Sato, Y., Matsumoto, K., Ogura, T. and Takahashi, Y. (1999). Coelom formation: binary decision of the lateral plate mesoderm is controlled by the ectoderm. *Development* **126**, 4129-4138.

George, E. L., Georges-Labouesse, E. N., Patel-King, R. S., Rayburn, H. and Hynes, R. O. (1993). Defects in mesoderm, neural tube and vascular development in mouse embryos lacking fibronectin. *Development* **119**, 1079-1091.

Goumans, M. J., Zwijsen, A., van Rooijen, M. A., Huylebroeck, D., Roelen, B. A. and Mummery, C. L. (1999). Transforming growth factor-beta signalling in extraembryonic mesoderm is required for yolk sac vasculogenesis in mice. *Development* **126**, 3473-3483.

Gurtner, G. C., Davis, V., Li, H., McCoy, M. J., Sharpe, A. and Cybulsky, M. I. (1995). Targeted disruption of the murine VCAM1 gene: essential role of VCAM-1 in chorioallantoic fusion and placentation. *Genes Dev.* **9**, 1-14.

Heldin, C. H., Miyazono, K. and ten Dijke, P. (1997). TGF-beta signalling from cell membrane to nucleus through SMAD proteins. *Nature* **390**, 465-471.

Hellqvist, M., Mahlapuu, M., Samuelsson, L., Enerback, S. and Carlsson, P. (1996). Differential activation of lung-specific genes by two forkhead proteins, FREAC-1 and FREAC-2. *J. Biol. Chem.* **271**, 4482-4490.

Kwee, L., Baldwin, H. S., Shen, H. M., Stewart, C. L., Buck, C., Buck, C. A. and Labow, M. A. (1995). Defective development of the embryonic and extraembryonic circulatory systems in vascular cell adhesion molecule (VCAM-1) deficient mice. *Development* **121**, 489-503.

Lawson, K. A., Dunn, N. R., Roelen, B. A., Zeinstra, L. M., Davis, A. M., Wright, C. V., Korving, J. P. and Hogan, B. L. (1999). Bmp4 is required for the generation of primordial germ cells in the mouse embryo. *Genes Dev.* **13**, 424-436.

Mahlapuu, M., Pelto-Huikko, M., Aitola, M., Enerback, S. and Carlsson, P. (1998). FREAC-1 contains a cell-type-specific transcriptional activation domain and is expressed in epithelial-mesenchymal interfaces [published erratum appears in *Dev. Biol.* **207**, 476]. *Dev. Biol.* **202**, 183-195.

Neufeld, G., Cohen, T., Gengrinovitch, S. and Poltorak, Z. (1999). Vascular endothelial growth factor (VEGF) and its receptors. *FASEB J.* **13**, 9-22.

Ogawa, M., Kizumoto, M., Nishikawa, S., Fujimoto, T., Kodama, H. and Nishikawa, S. I. (1999). Expression of alpha4-integrin defines the earliest precursor of hematopoietic cell lineage diverged from endothelial cells. *Blood* **93**, 1168-1177.

Oshima, M., Oshima, H. and Taketo, M. M. (1996). TGF-beta receptor type II deficiency results in defects of yolk sac hematopoiesis and vasculogenesis. *Dev. Biol.* **179**, 297-302.

Peterson, R. S., Lim, L., Ye, H., Zhou, H., Overdier, D. G. and Costa, R. H. (1997). The winged helix transcriptional activator HFH-8 is expressed in the mesoderm of the primitive streak stage of mouse embryos and its cellular derivatives. *Mech. Dev.* **69**, 53-69.

Pierrou, S., Hellqvist, M., Samuelsson, L., Enerback, S. and Carlsson, P. (1994). Cloning and characterization of seven human forkhead proteins: binding site specificity and DNA bending. *EMBO J.* **13**, 5002-5012.

Radice, G. L., Rayburn, H., Matsunami, H., Knudsen, K. A., Takeichi, M. and Hynes, R. O. (1997). Developmental defects in mouse embryos lacking N-cadherin. *Dev. Biol.* **181**, 64-78.

Risau, W. and Flamme, I. (1995). Vasculogenesis. *Annu. Rev. Cell Dev. Biol.* **11**, 73-91.

Sato, T. N., Tozawa, Y., Deutsch, U., Wolburg-Buchholz, K., Fujiwara, Y., Gendron-Maguire, M., Gridley, T., Wolburg, H., Risau, W. and Qin, Y. (1995). Distinct roles of the receptor tyrosine kinases Tie-1 and Tie-2 in blood vessel formation. *Nature* **376**, 70-74.

Shalaby, F., Rossant, J., Yamaguchi, T. P., Gertsenstein, M., Wu, X. F., Breitman, M. L. and Schuh, A. C. (1995). Failure of blood-island formation and vasculogenesis in Flk-1-deficient mice. *Nature* **376**, 62-66.

Tonegawa, A., Funayama, N., Ueno, N. and Takahashi, Y. (1997). Mesodermal subdivision along the mediolateral axis in chicken controlled by different concentrations of BMP-4. *Development* **124**, 1975-1984.

Tonegawa, A. and Takahashi, Y. (1998). Somitogenesis controlled by Noggin. *Dev. Biol.* **202**, 172-182.

Winnier, G., Blessing, M., Labosky, P. A. and Hogan, B. L. (1995). Bone morphogenetic protein-4 is required for mesoderm formation and patterning in the mouse. *Genes Dev.* **9**, 2105-2116.

Yamaguchi, T. P., Dumont, D. J., Conlon, R. A., Breitman, M. L. and Rossant, J. (1993). flk-1, an flt-related receptor tyrosine kinase is an early marker for endothelial cell precursors. *Development* **118**, 489-498.

Yang, J. T., Rayburn, H. and Hynes, R. O. (1993). Embryonic mesodermal defects in alpha 5 integrin-deficient mice. *Development* **119**, 1093-1105.

Yang, J. T., Rayburn, H. and Hynes, R. O. (1995). Cell adhesion events mediated by alpha 4 integrins are essential in placental and cardiac development. *Development* **121**, 549-560.